Atherosclerosis 219 (2011) 579–587

Atherosclerosis

journal homepage: www.elsevier.com/locate/atherosclerosis

Molecular imaging with optical coherence tomography using ligand-conjugated microparticles that detect activated endothelial cells: Rational design through target quantification

Andrew Jefferson[a], Rohan S. Wijesurendra[a], Martina A. McAteer[a], Janet E. Digby[a], Gillian Douglas[a], Thomas Bannister[a], Francisco Perez-Balderas[b], Zsolt Bagi[c], Alistair C. Lindsay[a], Robin P. Choudhury[a,*]

[a] Department of Cardiovascular Medicine and Oxford Acute Vascular Imaging Centre, University of Oxford, John Radcliffe Hospital, Oxford, OX3 9DU, United Kingdom
[b] Gray Institute for Radiation Oncology and Biology, University of Oxford, Old Road Campus Research Building, Oxford, OX3 7DQ, United Kingdom
[c] Department of Pharmacology, University of Oxford, Mansfield Road, Oxford, OX1 3QT, United Kingdom

ARTICLE INFO

Article history:
Received 5 May 2011
Received in revised form 27 July 2011
Accepted 28 July 2011
Available online 5 August 2011

Keywords:
Molecular imaging
OCT
Inflammation
Microparticles

ABSTRACT

Objectives: Optical coherence tomography (OCT) is a high resolution imaging technique used to assess superficial atherosclerotic plaque morphology. Utility of OCT may be enhanced by contrast agents targeting molecular mediators of inflammation.
Methods and results: Microparticles of iron oxide (MPIO; 1 and 4.5 μm diameter) in suspension were visualized and accurately quantified using a clinical optical coherence tomography system. Bound to PECAM-1 on a plane of cultured endothelial cells under static conditions, 1 μm MPIO were also readily detected by OCT. To design a molecular contrast probe that would bind activated endothelium under conditions of shear stress, we quantified the expression (basal *vs.* TNF-activated; molecules μm^{-2}) of VCAM-1 (not detected *vs.* 16 ± 1); PECAM-1 (132 ± 6 *vs.* 198 ± 10) and E-selectin (not detected *vs.* 46 ± 0.6) using quantitative flow cytometry. We then compared the retention of antibody-conjugated MPIO targeting each of these molecules plus a combined VCAM-1 and E-selectin (E + V) probe across a range of physiologically relevant shear stresses. E + V MPIO were consistently retained with highest efficiency ($P < 0.001$) and at a density that provided conspicuous contrast effects on OCT pullback.
Conclusion: Microparticles of iron oxide were detectable using a clinical OCT system. Assessment of binding under flow conditions recommended an approach that targeted both E-selectin and VCAM-1. Bound to HUVEC under conditions of flow, targeted 1 μm E + V MPIO were readily identified on OCT pullback. Molecular imaging with OCT may be feasible *in vivo* using antibody targeted MPIO.

1. Introduction

Optical coherence tomography (OCT) is a high-resolution optical imaging technique with a range of applications in biology and medicine. Using a wire-mounted endovascular near-infrared probe, the walls of coronary arteries can be imaged with high resolution (~10 μm), though with relatively limited depth penetrance. Consequently, OCT is used to evaluate superficial atherosclerotic plaque morphology [1], including macrophage accumulation [2]. The utility of OCT might be further enhanced by the availability of molecular imaging contrast agents directed towards targets that are differentially expressed in pathological states by the vascular endothelium. Successful molecular imaging approaches have used reporter particles that include ligand-conjugated microbubbles [3], micelles [4], liposomes [5] and iron oxide-containing micro- [6] or nanoparticles [7]. Effective contrast agents for OCT enhance light scattering, for instance through the use of gold- [8,9] or titanium dioxide nanoparticles [10]. Microparticles of iron oxide (MPIO) also exert a light scattering effect [11], though they have not been tested as a monolayer that would be required for vascular molecular imaging.

Molecules upregulated in vascular inflammation (such as VCAM-1 [12] and E-selectin [13]) mediate leukocyte adhesion to activated endothelium and provide an attractive target for imaging and drug delivery. Their prominent position on the luminal surface of endothelial cells allows ready access to circulating ligand–particle complexes. Such markers have been targeted most commonly with antibodies, although peptide–protein recognition and carbohydrate–protein binding provide alternative strategies

* Corresponding author at: Department of Cardiovascular Medicine, Level 6, West Wing, John Radcliffe Hospital, Oxford. OX3 9DU, United Kingdom.
Tel.: +44 1865 234663; fax: +44 1865 234667.
E-mail address: robin.choudhury@cardiov.ox.ac.uk (R.P. Choudhury).

0021-9150
doi:10.1016/j.atherosclerosis.2011.07.127

[14,15]. However, a major challenge is the delivery of a targeted particulate contrast agent to the endothelial surface in sufficient quantities under conditions of high shear stress to permit its identification. Critical to the rational design of such contrast agents is knowledge of (1) the abundance of these targets, (2) the extent to which their surface expression varies between basal and activated states, and (3) the ability of contrast particles to bind under conditions of flow.

Here, we investigate the potency of MPIO targeted to human PECAM-1, VCAM-1 or E-selectin or a combination of VCAM-1 and E-selectin to bind to stimulated human endothelial cells under a range of shear stress conditions. Using these findings, we then applied a catheter-mounted clinical OCT system to visualize and quantify MPIO binding to activated endothelial cells *in vitro* under physiologically relevant conditions of shear stress to demonstrate the possibility of OCT for molecular imaging of vascular inflammation.

2. Materials and methods

2.1. Cell culture

Primary human umbilical vein endothelial cells (HUVEC, Invitrogen, Paisley, UK) were cultured in Medium 200 supplemented with low-serum growth supplement (LSGS) (Invitrogen). Cells were used between passages 2 and 5, and when required, stimulated with recombinant human tumour necrosis factor-α (TNF-α) (Invitrogen) at a concentration of 10 ng mL^{-1}.

2.2. Antibody–MPIO conjugation

Mouse anti-human monoclonal antibodies against VCAM-1 (Clone 4B2), E-selectin (5D11) and PECAM-1 (9G11) (R&D Systems, Abingdon, UK) and an isotype control rat monoclonal IgG_2 (G2a-1-1) (Southern Biotechnology, Birmingham, USA) antibody (50 μg for each) were covalently conjugated to ~1.25×10^9, 1 μm tosyl-activated Dynalbeads (MPIO) (Invitrogen). For dual-labelled E-selectin + VCAM-1 (E + V) MPIO, 25 μg of each antibody was added to a labelling reaction to give a total of 50 μg (as previously described [16]).

2.3. Immunocytochemistry and MPIO staining

HUVEC grown on poly-D-lysine coated glass were stimulated with TNF-α for 8 h, washed with PBS and fixed in methanol-free formaldehyde 4% for 10 min. For immunostaining, cells were blocked with 3% BSA. Antibodies to human VCAM-1, E-selectin and PECAM-1 were incubated with cells at 4 °C overnight (final concentration 20 μg mL^{-1}) and, after washing, incubated with goat anti-mouse Alexa Fluor 488 (Invitrogen) (5 μg mL^{-1}) for 30 min at 37 °C. After a final wash in PBS, coverslips were mounted on a standard microscope slide in *SlowFade* Gold antifade reagent with 4′,6-diamidino-2-phenylindole (Invitrogen). Antibody-attachment to MPIO was confirmed by incubating 50 ng of antibody–MPIO with goat anti-mouse Alexa Fluor 488 (1 μg mL^{-1}) for 30 min at 37 °C. An Olympus IX-71 inverted microscope fitted with a 100×, 1.3 NA oil immersion objective (Olympus UK, Southend-on-Sea, UK), and a QICAM cooled monochrome CCD camera (QImaging, Surrey, Canada) driven using ImagePro-Plus (Media Cybernetics, Bethesda, USA) were used.

2.4. RNA extraction and RT-PCR

Quantitative real-time RT-PCR was used to measure expression of VCAM-1 (CD106), E-selectin (CD62E) and PECAM-1 (CD31) in HUVEC under basal conditions and after TNF-α-stimulation, using GAPDH as a normalization gene. Following stimulation with TNF-α for 4 h, RNA was extracted using an RNeasy Mini Kit (Qiagen, Crawley, UK) and cDNA was synthesised using a QuantiTect reverse transcription kit (Qiagen). TaqMan™ primers for VCAM-1, E-selectin, PECAM-1 and GAPDH were used to amplify cDNA on a StepOne PCR system (Applied Biosystems, Warrington, UK). Relative quantities of mRNA expressed in arbitrary units were calculated using the $2^{\Delta\Delta Ct}$-method [17].

2.5. Quantitative flow cytometry to establish relative ligand abundance

Qifikit calibration beads (Dako, Ely, UK) were used as a reference to determine ligand density from fluorescence intensity. HUVEC were stimulated with TNF-α for 8 h, washed with PBS and detached using non-enzymatic cell dissociation solution (Sigma, Poole, UK). The cells were centrifuged (1200 rpm; 5 min) and resuspended in 100 μL PBS. Primary antibodies to VCAM-1, E-selectin and PECAM-1 and an irrelevant mouse monoclonal anti-human CD68 (R&D Systems) were added at a final concentration of 10 μg mL^{-1}. Anti-mouse-FITC conjugate (Qifikit, Dako) was added at a dilution of 1:50. Flow cytometry experiments were performed on a BD LSRII flow cytometer and the data analysed using Cytobank (www.cytobank.org).

2.6. Quantitative flow cytometry to establish antibody loading on MPIO

Antibody–MPIO conjugates (~2.5×10^6 MPIO mL^{-1}) were labelled in suspension with secondary antibody. Alexa Fluor 488 for IgG_2, was added at a 200× excess relative to the primary antibody. The standard curve generated above was used to calculate antibody loading density on MPIO.

2.7. Antibody–MPIO binding experiments under static and shear stress conditions

HUVEC were stimulated with TNF-α for 8 h, fixed with 4% formaldehyde, washed with PBS and stored at 4 °C. For static binding experiments, antibody–MPIO (10 μg mL^{-1} antibody; ~2.5×10^8 MPIO mL^{-1}) was added to cells and placed on a benchtop rocker prior to thorough washing with PBS. Binding under shear stress was performed by mounting culture dishes on a Parallel-Plate flow chamber (GlycoTech, Gaithersburg, USA) fitted with gasket B (0.25 cm × 0.025 cm) and connected to a syringe infusion pump (Pump 22; Harvard Apparatus, Cambridge, USA).

Flow rates to generate the required shear stress conditions were calculated using the following formula $\tau = 6Q\mu/bh^2$, whereby τ = shear stress (dyne cm^{-2}), Q = flow rate (mL s^{-1}), μ = viscosity of liquid (in poise (P); dH_2O = 0.0076 P), b = channel width (cm) and h = channel height (cm). To simulate a range of physiological shear stress conditions that are found in the circulatory system, flow chamber experiments were conducted at 1, 5, 10 and 15 dyne cm^{-2}. MPIO binding after 5 min of shear stress was assessed in 20 random fields of view in 4 separate experiments using a 40×, 0.6 NA objective fitted to the Olympus IX-71 microscope described above. Clumps of MPIO were counted as a single binding event.

2.8. Assessment of MPIO binding in ex vivo coronary arterioles

Ex vivo, cannulated and pressurized coronary arterioles were studied with bright field and fluorescence videomicroscopy, as described previously [18,19]. Briefly, with the use of microsurgical instruments and an operating microscope, the second branch of septal coronary arteriole (internal diameter 125–150 μm and ~1.5 mm in length) was isolated from the heart of male Wistar rats (N = 4) and transferred to organ chambers containing two glass

micropipettes filled with MOPS (pH 7.4). The vessels were cannulated at both ends, and the micropipettes were connected with silicone tubing to hydrostatic pressure reservoirs to set the intraluminal pressure to 70 mmHg. The temperature was set at 37 °C by a circulating bath temperature controller (Grant Instruments, Cambridge, UK).

VCAM-1 MPIO were prepared as described above and administered intraluminally to the coronary arteriole at constant flow rate of 25 μL min^{-1}. Intraluminal flow was generated by changing the inflow and outflow pressures in opposite direction, while flow rate was measured with a ball-type flow meter (Omega, Stamford, USA). The arteriolar diameter was continuously recorded and wall shear stress was calculated, as described earlier [20].

MPIOs were visualized with whole-field fluorescence measurements by using a ultra fast filter switching-based imaging system (Oligochrome, TILL Photonics, Uckfield, UK) on a Nikon Eclipse FN1 microscope (Nikon, Kingston-upon-Thames, UK) equipped with a 20× water dipping objective (NA 0.5) and illuminated with 475/35 nm light. Fluorescent images were acquired with an Andor Luca (S) cooled EM CCD camera (Andor, Belfast, Northern Ireland) at 10 Hz. Images were analysed off-line using Arivis Browser (TILL Photonics). Small regions of interest (1000 μm^2) were selected over the surface of endothelial layer and MPIOs were counted manually. The number of bound MPIO were averaged in these regions and presented as binding events per 1000 μm^2.

Following basal flow experiments, *ex vivo* coronary arterioles were stimulated with TNF-α (7.25 nmol L^{-1}, for 4 h) and MPIO binding events were recorded after stimulation.

2.9. Western immunoblotting

Single coronary arterioles (1 vessel from each animal) were dissected from the heart of Wistar rats. Cleared of connective tissue and placed into MOPS (37 °C, pH 7.4). Coronary arterioles were incubated with or without TNF-α (7.25 nmol L^{-1}) for 4 h and then vessels were snap-frozen in liquid nitrogen. Arterioles were homogenized in 20 μL ice-cold RIPA buffer (Sigma) and additional 20 μL of Laemmli buffer were added (Sigma) and SDS electrophoresis and consequent immunoblot analysis was carried out as described earlier [18]. Anti-VCAM-1 and anti-β-actin primary and respective horseradish peroxidise-labelled secondary antibodies were used for protein detection. Signals were revealed with chemiluminescence and visualized autoradiographically.

2.10. MPIO phantom and flow chamber dish preparation for OCT imaging

Suspensions of MPIO in 0.4% agarose were prepared in glass tubes at densities of 3, 2 and 0.12×10^6 MPIO mL^{-1} for 4.5 μm MPIO, and 5 and 2.5×10^8 MPIO mL^{-1} for 1 μm MPIO.

For monolayer experiments, PECAM-1–MPIO (1 μm) were added to a dish of fixed HUVEC and incubated under static conditions described above. A 20-gauge venous cannula (BD Biosciences) provided a track for the OCT catheter immediately above the cell monolayer. E + V–MPIO were run through the flow chamber at shear stresses of 1 and 5 dyne cm^{-2}.

OCT was performed using a C7 Dragonfly Catheter connected to a C7-XR OCT Intravascular Imaging System (LightLab, St Paul, USA). A 15 mm pullback (0.5 mm s^{-1}) was used to image bound antibody–MPIO. The signal or contrast generated by the MPIO was measured by thresholding the images to a pixel intensity 2 standard deviations above the background, and then measuring the area of signal above threshold using ImageJ (NIH, Bethesda, USA).

2.11. Statistical analysis

Two-tailed, unpaired Student's *t*-tests were used for all statistical comparisons.

3. Results

3.1. Optical coherence tomography characteristics of MPIO

MPIO dispersed in suspension produced a light scattering effect represented as discreet regions of bright signal in the OCT image. Larger MPIO resulted in brighter and more distinct signal, with the 4.5 μm particles conspicuous as punctuate spots. The 1 μm MPIO were clearly detectable above background, though in a more diffuse pattern (Fig. 1).

OCT was next applied to image MPIO in a single plane on a monolayer of endothelial cells, rather than suspended in a volume. PECAM-1-targeted 1 μm MPIO were allowed to bind under static conditions to a monolayer of HUVEC, which constitutively express PECAM-1, represented in Fig. 2A. Bound MPIO appeared as an intensely bright band along the cell surface (Fig. 2B), with homogeneous low signal in the 'no-MPIO' control (Fig. 2C). The signal intensity profile of a line drawn across the monolayer (Fig. 2D) shows clear demarcation of MPIO from adjacent cells/agarose. This marked contrast effect was consistent along a 10 mm automated pullback and a significant difference in the mean pixel intensity was observed between PECAM-1–MPIO and no MPIO controls (Fig. 2E).

3.2. Expression of inflammatory markers in cell model

Immunocytochemistry demonstrated endothelial localisation of VCAM-1 and E-selectin in TNF-α stimulated cells and PECAM-1 in both basal and activated states (Supplementary Fig. 1A–C). Real-time quantitative RT-PCR showed marked TNF-α induced expression of VCAM-1 and E-selectin in HUVEC cultures compared to the basal state. PECAM-1 was constitutively expressed, with comparable mRNA levels in stimulated and basal HUVEC (Supplementary Fig. 1D–F).

3.3. Quantitative flow cytometry to establish target abundance on endothelial cells

In the basal state, VCAM-1 and E-selectin were undetectable, while PECAM-1 was present at 132 ± 6 molecules μm^{-2}. In TNF-α stimulated cells, VCAM-1 and E-selectin were expressed, at ligand densities of 16 ± 1 and 46 ± 0.6 molecules μm^{-2}, respectively, and PECAM-1 density rose to 198 ± 10 molecules μm^{-2}. The anti-CD68 control was negative under each condition (Supplementary Table 1 and Fig. 2). The density of E-selectin was significantly greater than that of VCAM-1 ($P = 0.001$), while the density of PECAM-1 was significantly greater than both inducible markers ($P \leq 0.002$).

3.4. Quantitative flow cytometry to establish antibody density on MPIO

Loading densities of VCAM-1, E-selectin, PECAM-1 and IgG_2 antibodies conjugated to 1 μm MPIO were also assessed. Fluorescence intensity histograms generated from flow cytometry analysis of antibody-labelled MPIO (Supplementary Fig. 3) suggested that 90–95% of MPIO were labelled with antibody. The density was calculated to be 27,100 ± 1920 molecules per MPIO for all antibodies; equivalent to 8500 molecules μm^{-2}. Therefore, the ligand density on the MPIO far exceeds the target density on the cell; a fundamental pre-requisite if MPIO binding is to be used for target quantification.

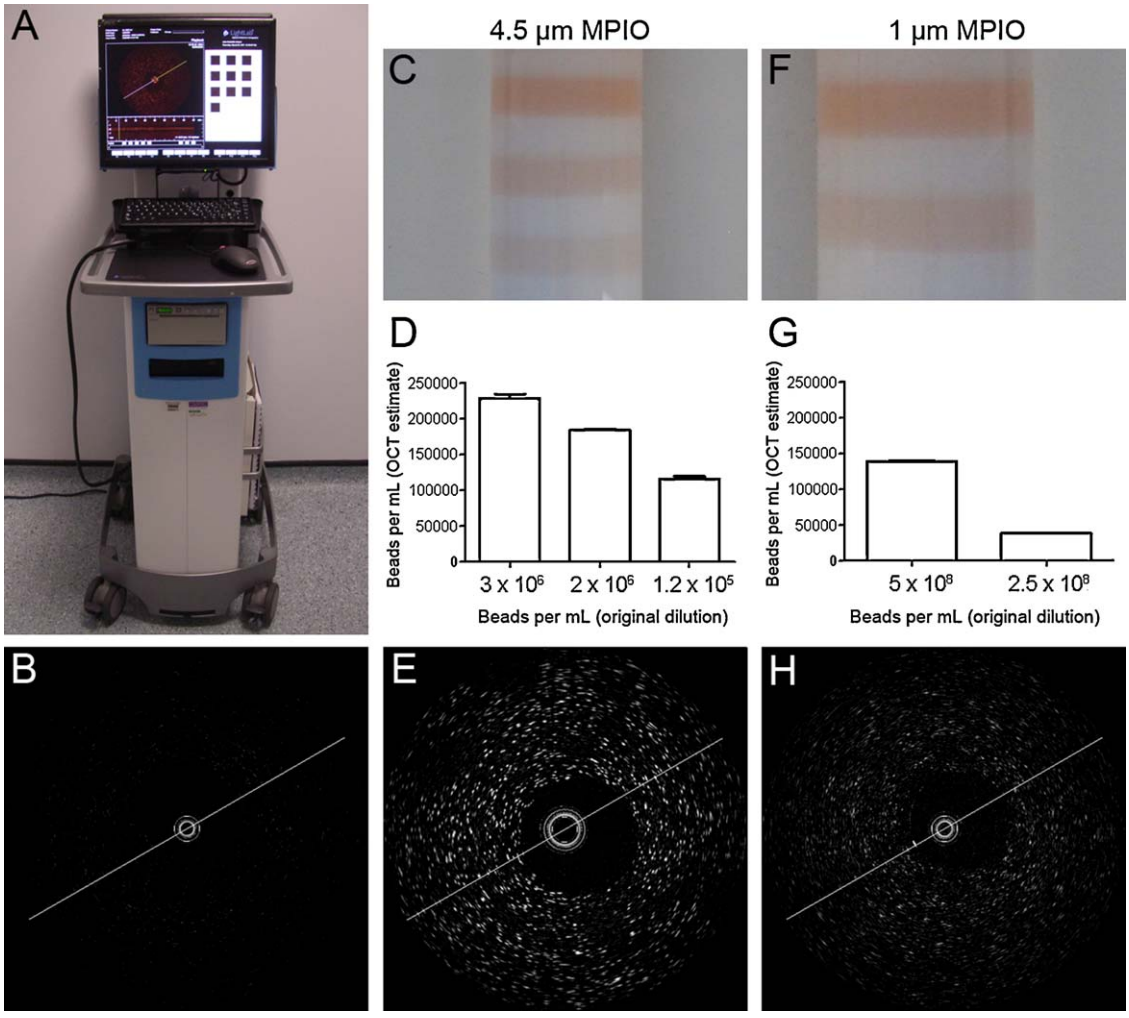

Fig. 1. Contrast optical coherence tomography. The commercially available LightLab C7-XR OCT Intravascular Imaging System used in this study (A). Optical coherence tomography reveals minimal background scatter (B) of the 0.4% agarose used in the preparation of MPIO phantoms. 4.5 μm MPIO at variable concentration in an arterial phantom (C) were quantifiable using automated analysis of OCT data (D), and visible as punctuate spots in the image (E). 1 μm MPIO in a phantom (F) were also quantifiable (G), and visible as punctuate spots in the image (H).

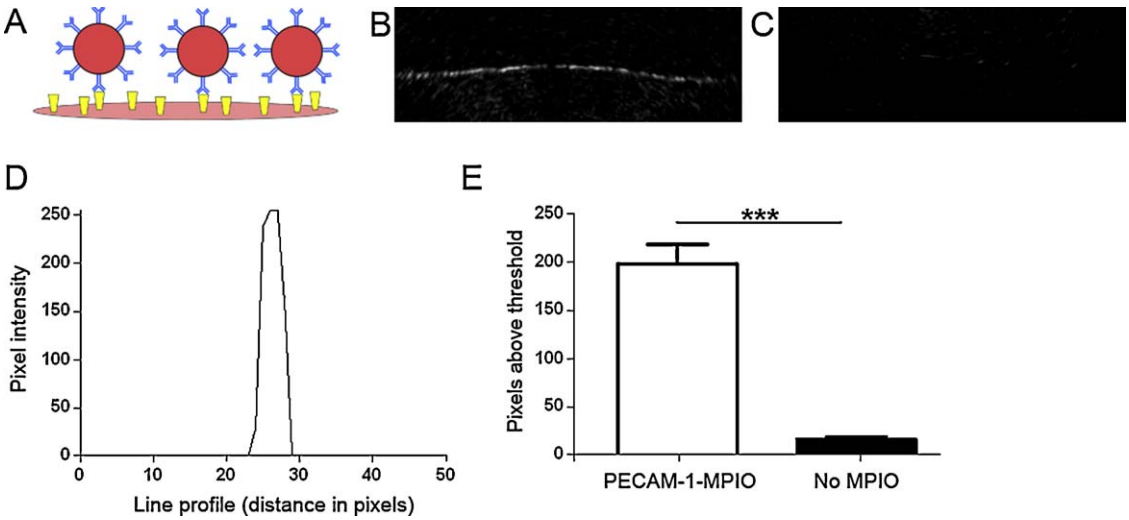

Fig. 2. Optical coherence tomography of MPIO on a cell monolayer. (A) A cartoon representation of antibody-labelled MPIO [red] binding to endothelial cell surface markers [yellow]. The PECAM-1–MPIO bound to the cell monolayer are visible as a bright horizontal band in the OCT image (B). 'No-MPIO' control experiment confirms background signal is minimal (C). The intensity profile of a line drawn perpendicular to the monolayer with PECAM-1–MPIO bound reveals a clear demarcation between MPIO and surrounding agarose and cells (D). Areas of measurable signal along the pullback are significantly greater for PECAM-1–MPIO compared with the no MPIO control (E) (Error bars represent ±1 SEM). (For interpretation of the references to color in this figure legend, the reader is referred to the web version of the article.)

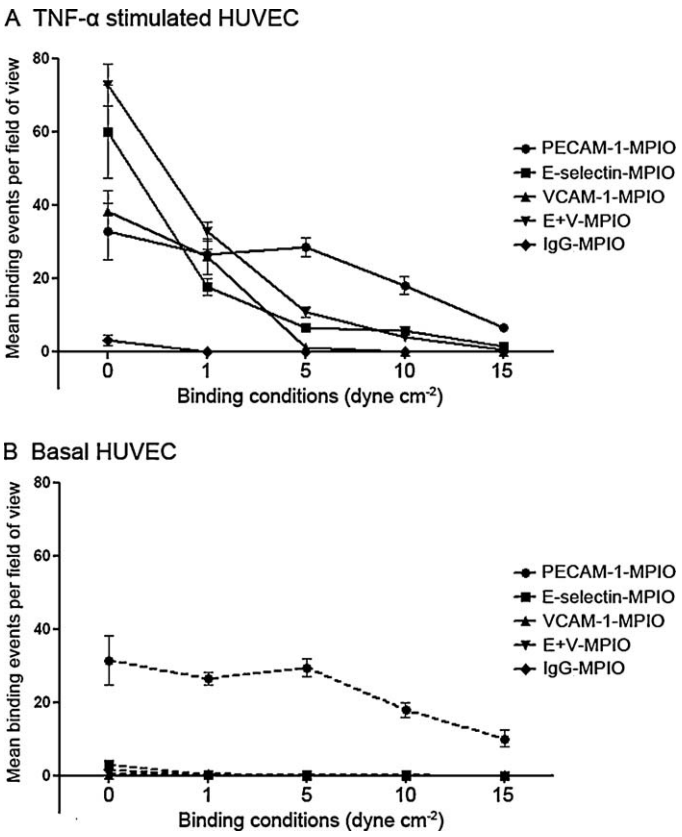

Fig. 3. Binding of E-selectin-, VCAM-1-, E + V-, PECAM-1- and IgG_2–MPIO to TNF-α stimulated and basal HUVEC. In stimulated cells under static and low shear stress conditions, antibody–MPIO to E-selectin, VCAM-1 and E + V bind in greater numbers than PECAM-1–MPIO. However, as shear stress increases, PECAM-1–MPIO bind in significantly greater numbers than the other antibody–MPIO (A). In basal cells, only antibody–MPIO targeted to the constitutively expressed PECAM-1 are able to bind above background (B).
Data points are expressed as mean MPIO bound per field of view (MPIO/fov), with error bars representing ±1 SEM.

3.5. Antibody-conjugated-MPIO binding under static conditions

In basal state, there was sparse retention of MPIO targeting E-selectin, VCAM-1, E-selectin + VCAM-1 in combination ("E + V") and the IgG_2 negative control. Conversely PECAM-1–MPIO bound abundantly even in basal state. TNF-α-stimulation greatly increased binding for E-selectin, VCAM-1 and 'E + V' but was unchanged for both PECAM-1 and the IgG_2 negative control, consistent with upregulation of E-selectin and VCAM-1 under cytokine stimulation (Tale 1 and Fig. 3). Binding of E + V–MPIO was significantly higher than all other antibody–MPIO tested ($P < 0.001$). E-selectin–MPIO bound significantly more than both VCAM-1- and PECAM-1–MPIO ($P = 0.004$). There was no significant difference between binding of VCAM-1- and PECAM-1–MPIO under static conditions ($P = 0.26$).

3.6. Antibody–MPIO binding under conditions of shear stress

In general, antibody–MPIO binding fell as shear stress increased; the binding of antibody–MPIO seen at 1 dyne cm^{-2} greatly reduced upon increasing shear stress to 5 dyne cm^{-2} and higher, particularly that of VCAM-1–MPIO. In the like-for-like comparison, E-selectin–MPIO generally bound in greater numbers than VCAM-1–MPIO. Of particular note, the dual-labelled E + V–MPIO bound in significantly higher numbers than all other antibody–MPIO targeting inducible mediators of inflammation ($P < 0.001$ for all), with the exception of binding slightly less than E-selectin–MPIO at 10 dyne cm^{-2}, suggesting a synergistic effect of antibodies to different targets on a single MPIO. In keeping with the observations under static conditions (above), minimal binding of E-selectin-, VCAM-1-, E + V- and IgG_2–MPIO was observed in basal cells. PECAM-1–MPIO, while not indicative of activated endothelium, bound in higher numbers at higher shear stress than the other antibody–MPIO.

3.7. MPIO binding in ex vivo coronary arterioles

VCAM-1–MPIO were delivered intraluminally into isolated, pressurized arterioles at constant flow rate of 25 μL min^{-1}. The 25 μL min^{-1} flow elicited 5–10 dyne cm^{-2} wall shear stress in 125–150 μm diameter arterioles, close to shear stress levels to which these vessels are exposed *in vivo*. Under these conditions we detected real-time firm binding of VCAM-1–MPIO (Fig. 4A and B and Movie), events that were enhanced when coronary arterioles were exposed to TNF-α. Correspondingly, TNF-α stimulation resulted in an increased protein expression of VCAM-1 in coronary arterioles (Fig. 4C).

3.8. Optical coherence tomography of MPIO bound under shear stress

In order to assess the capability of OCT to image targeted MPIO on a monolayer at physiologically relevant retention levels, E + V–MPIO were exposed to TNF-α-stimulated HUVEC with non-stimulated cells as a negative control. E + V–MPIO bound to stimulated cells at 1 dyne cm^{-2} could be identified using OCT, by measuring pixel area above a threshold set to 2 standard deviations above background. Despite the variability in MPIO signal along the pullback, a substantial difference was observed between E + V–MPIO on stimulated cells *vs.* on basal (107 pixels above threshold ± 33 *vs.* 18 pixels ± 22; $P < 0.0001$). At 5 dyne cm^{-2} binding of E + V–MPIO was diminished but was 2.5-fold greater than the negative control (42 pixels ± 45 *vs.* 16 pixels ± 13; $P = 0.0012$) (Fig. 5).

4. Discussion

Optical coherence tomography provides high-resolution anatomical images of coronary arteries and associated pathology. Here, we designed and evaluated *in vitro* a new molecular OCT imaging agent targeting molecules that are differentially expressed by activated endothelial cells. Light-scattering particles of iron oxide provided conspicuous contrast when bound to the activated endothelium under conditions of shear stress that were designed to mimic *in vivo* binding.

To date, a range of particles have been used to enhance signal for OCT. Gold nanoparticles demonstrate a light scattering effect [9] and immuno-targeting has allowed them to be used in live cell studies [21]. Particles of iron oxide have excellent light scattering properties [11]. Furthermore, the surfaces of such particles can be functionalised to allow loading with specific ligands targeting vascular endothelium [16]. As expected, the light scattering and therefore contrast effects of larger particles were greater, but even 1 μm MPIO were readily identifiable with OCT. However, given the known tendency for ≥4.5 μm particles to be retained by the lungs after intra-venous injection [16], we elected to evaluate the smaller (1 μm) MPIO in subsequent experiments.

A number of imaging and therapeutic approaches have successfully targeted adhesion molecules that are involved in the recruitment of circulating leukocytes to sites of local inflammation [3,6,22]. While the roles of adhesion molecules in cellular recruitment have been partially defined [15], their relative abilities to mediate binding of antibody-conjugated inert particles is

Table 1
Antibody–MPIO binding to endothelial markers under static and shear stress conditions.

Antibody–MPIO	Binding conditions	TNF-α stimulated HUVEC		Basal HUVEC	
		Binding events per fov	SEM	Binding events per fov	SEM
E-Selectin	Static	60	6.5	3.1	0.6
VCAM-1		38	2.8	0.33	0.4
E + V		73	2.9	0.6	0.2
PECAM-1		33	4	32	3.4
IgG_2		3	0.7	1.65	0.5
E-selectin	1 dyne cm^{-2}	18	1.2	0.2	0.07
VCAM-1		26	2.5	0.625	0.2
E + V		33	1.3	0.45	0.09
PECAM-1		27	0.7	27	0.8
IgG_2		0.13	0.04	0.2	0.06
E-selectin	5 dyne cm^{-2}	6.3	0.6	0.1	0.08
VCAM-1		1.1	0.2	0.01	0.02
E + V		10.9	0.8	0.2	0.1
PECAM-1		29	1.3	30	1.2
IgG_2		0.04	0.05	0.03	0.05
E-selectin	10 dyne cm^{-2}	5.7	0.6	0.075	0.07
VCAM-1		0.1	0.05	0.0125	0.02
E + V		4	0.3	0.2	0.1
PECAM-1		18	1.2	18	1
IgG_2		0.04	0.05	0.03	0.03
E-selectin	15 dyne cm^{-2}	1.45	0.4	0.03	0.03
VCAM-1		0.09	0.08	0.04	0.04
E + V		0.7	0.3	0.04	0.04
PECAM-1		6.6	1.0	10.2	2.3
IgG_2		0.075	0.08	0.05	0.06

unexplored. To fully capitalise on these properties, requires appreciation of (a) the density of the target and (b) the extent to which its expression changes between basal and activated states and (c) the relative affinities of ligand and ligand combinations for these targets, including under conditions of shear stress.

While PECAM-1 was the most abundant target molecule, this study confirmed its constitutive expression and lack of regulation in response to a pro-inflammatory stimulus. In contrast, both E-selectin and VCAM-1 were markedly up-regulated from undetectable levels, and therefore more suitable as targets for

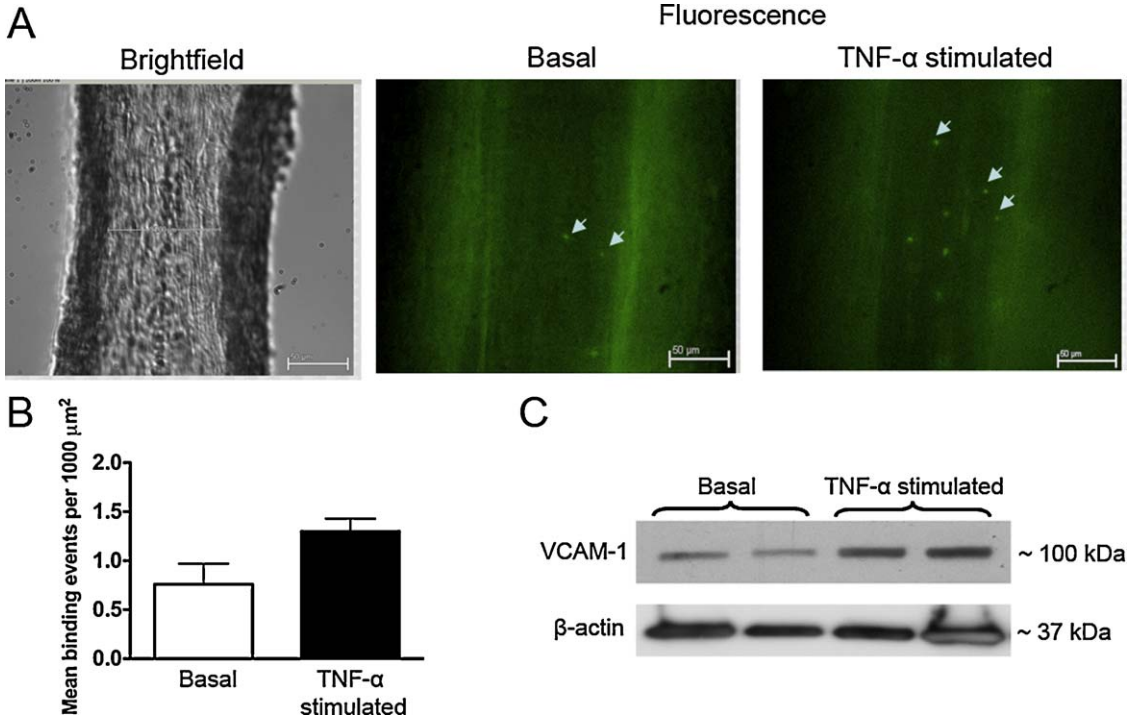

Fig. 4. Representative microphotographs show isolated, pressurized coronary arterioles (internal diameter: 100 μm) of the rat. Left panel shows bright field image of the arteriole, whereas fluorescent (FITC excited) images show VCAM-1–MPIO (arrowheads) adhered to the endothelial cells before (basal, shown in the middle panel) and after stimulation with TNF-α (7.25 nmol L^{-1} for 4-h, right panel). VCAM-1–MPIO were delivered intraluminally into the pressurized arteriole at the flow rate of 25 μL min^{-1} (A). Mean binding events in isolated coronary arterioles were significantly higher in TNF-α stimulated vessel than in basal tissue (B). Western immunoblots show expression of VCAM-1 and β-actin in coronary arterioles before (basal) and after stimulation with TNF-α (7.25 nmol L^{-1} for 4-h).

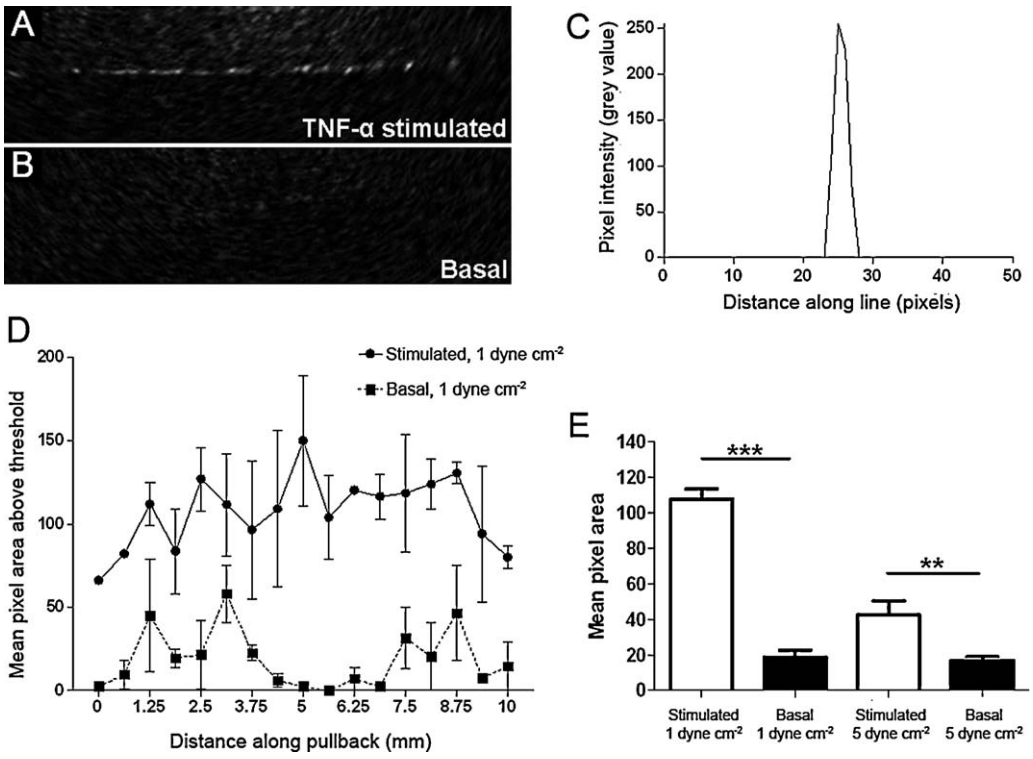

Fig. 5. OCT imaging of MPIO binding to E-selectin and VCAM-1 under conditions of shear stress. Binding of E + V–MPIO at 1 dyne cm^{-2} was detectable using OCT, and the particles bound to the cell monolayer were clearly visible (A). No signal was seen in the basal control at 1 dyne cm^{-2} (B). The intensity profile of a line drawn perpendicular to the monolayer with PECAM-1–MPIO bound reveals a clear demarcation between MPIO and surrounding agarose and cells (C). Area of signal generated by the E + V–MPIO binding at 1 dyne cm^{-2} in the OCT images is significantly higher in the stimulated cells than in the basal controls (D&E), while the reduction in binding to stimulated cells at 5 dyne cm^{-2} results in a lower signal area, but which is still significantly greater than the basal equivalent (E). Error bars represent ±1 SEM.

distinguishing pathological states. The design of a contrast agent should take into consideration the abundance and location of the target. Based on our findings, targets at a low abundance may only be detectable by particles at relatively low shear stress, while higher abundance targets may be detected across a broader range of shear stress conditions.

The dynamics of leukocyte–endothelial binding are complex and dependent on multiple receptor–ligand interactions. Initial leukocyte rolling is selectin-mediated while firm adhesion is mediated by integrin binding to ICAM-1 and VCAM-1, with the latter more important in initiation of atherosclerosis. 'Adhesion dynamic modelling' predicts synergistic roles for selectins and integrins with transition between rolling and firm adhesion dependent on binding affinities and relative concentrations of receptor–ligand interactions [23,24]. Taking this into consideration, we have previously adopted a dual antibody-conjugated MPIO approach for targeted MRI and applied this to the detection of adhesion molecules on the arterial endothelium of apolipoprotein E knockout ($apoE^{-/-}$) mice *in vivo* [16]. The current *in vitro* data corroborate this: the E-selectin and VCAM-1 antibodies on the dual labelled MPIO combined synergistically to enhance particle binding across a wide range of shear stress conditions compared with the constituent single-targeted particles. Our dual-labelled E + V MPIO bound in sufficient numbers to allow detection with OCT enabling distinction of activated and basal endothelium under shear stress conditions that are representative of venous to arterial blood flow.

We corroborated our *in vitro* findings with an *ex vivo* experiment using rat coronary arterioles as a model of inflammation. Using fluorescently labelled VCAM-1–MPIO, we demonstrated the capacity of targeted MPIO to differentiate between inflamed and basal endothelium under conditions of shear stress.

We developed a cell-based *in vitro* model because of the ability to isolate and control variables influencing antibody–MPIO binding. We have previously reported binding of MPIO in mouse atherosclerosis, acute brain inflammation and in brain and renal ischemia–reperfusion injury, and the ability of MPIO to bind under conditions of flow, *in vivo*, is established [6,16]. *In vivo*, however, multiple variables may contribute to differential binding of MPIO, including: (1) ligand–target pairing; (2) target density; (3) shear forces; (4) specific anatomy. The purpose of the current approach was to vary (a) shear and (b) ligand–target pairing in a controlled fashion and to evaluate the contributions of each, thereby aiding rational contrast agent design. HUVEC were selected as they are a well-characterised model of inflammation [25,26] that have been previously used in leukocyte adhesion assays [27,28].

4.1. Limitations

This study and others have employed antibodies as targeting ligands. While antibodies can provide both high affinity and specificity, they are not the endogenous ligands for either integrins or selectins and our findings cannot be extrapolated to the binding of leukocytes *in vivo*. Nor can the results, with the specific antibodies used in this study, be generalised to all antibodies-target interactions, since variation in epitope and affinity may affect binding properties. Furthermore, antibodies are expensive to produce, and are capable of inducing an immune response in the host, so "humanisation" of animal antibodies would be required for safe use of such MPIO in humans. For these reasons alternative targeting strategies are under development. Recently, synthetic sialyl $Lewis^x$, a carbohydrate found on the surface of most leukocyte populations, has been used to target glyconanoparticles to E- and P-selectin in brain inflammation and a VCAM-1 specific peptide, generated by

phage display [29,30] has also been successfully used as a targeting molecule to image inflammatory atherosclerosis.

4.2. Imaging of MPIO endothelial targeted MPIO using OCT

MPIO bound to activated endothelium under conditions of shear stress were clearly identified. The *in vitro* system comprising of the monolayer of cells and agarose provided minimal background scattering with OCT and so despite the MPIO signal variability, a clear and statistically significant demarcation could be made between the presence or absence of bound MPIO, reflective of the inflamed or basal states. The *in vivo* environment and presence of different tissues, however, may produce more scattering, although unlabelled gold-coated protein microspheres been visualized via OCT in murine liver with minimal scatter from the native vasculature.

Should background scatter prove problematic, developments or refinements to the OCT protocol may improve the signal or contrast effect of imaging particles. For instance, differential phase-OCT has been described, whereby magnetic microparticles were excited by the application of an oscillating magnetic flux density and the improved contrast effect used to image macrophage infiltration in atherosclerotic plaque [31] and this technique would be directly applicable when targeted MPIO are used. Larger diameter microparticles provide enhanced scattering effects over smaller particles, but they may be undesirable in other aspects [16]; smaller particles decorated with optically active elements are also under investigation. In addition to quantification of molecular expression from the use of targeted imaging agent, OCT also provides complementary high-resolution morphological information on vessel and plaque structure [1]. OCT could be combined with non-invasive MR imaging to provide a hybrid imaging strategy; inflammation and plaque formation could first be identified using MRI, which could then be followed up with OCT at the time of coronary intervention to further characterise the plaque composition and morphology.

5. Conclusions

Microparticles of iron oxide (1 and 4.5 μm) were detectable using a commercially available optical coherence tomography system and imaging probe. Functionalised particles bearing antibodies to a range of endothelial targets were generated. Quantification of targets (E-selectin, VCAM-1 and PECAM-1) in cultured endothelial cells in a basal state and after TNF-α stimulation identified potential targets for molecular imaging. Assessment of binding under flow conditions recommended a combined approach that targeted both E-selectin and VCAM-1, as predicted from earlier *in silico* modelling and *in vivo* binding in mice. Bound under conditions of flow, targeted MPIO were readily identified on OCT pullback. Molecular imaging with OCT may be feasible *in vivo* using antibody targeted MPIO and combined with MR imaging to provide hybrid imaging approaches.

Acknowledgments

This research is supported by the British Heart Foundation. RPC is a Wellcome Trust Senior Research Fellow in Clinical Science. The study was supported by the Oxford Comprehensive Biomedical Research Centre, NIHR funding scheme. RPC and ZB acknowledge the support of the BHF Centre of Research Excellence, Oxford (RE/08/004). FP-B is supported by a Cancer Research UK Programme Grant (C28461; PI: Dr. N. R. Sibson). Flow Cytometry experiments were performed in the Oxford BRC Translational Immunology Laboratory. The BRC Immunology SRL is supported by the NIHR BRC. Phil Townsend is gratefully acknowledged for his general laboratory management.

Appendix A. Supplementary data

Supplementary data associated with this article can be found, in the online version, at doi:10.1016/j.atherosclerosis.2011.07.127.

References

[1] Yabushita H, Bouma BE, Houser SL, et al. Characterization of human atherosclerosis by optical coherence tomography. Circulation 2002;106:1640–5.
[2] Tearney GJ, Yabushita H, Houser SL, et al. Quantification of macrophage content in atherosclerotic plaques by optical coherence tomography. Circulation 2003;107:113–9.
[3] Villanueva FS, Jankowski RJ, Klibanov S, et al. Microbubbles targeted to intercellular adhesion molecule-1 bind to activated coronary artery endothelial cells. Circulation 1998;98:1–5.
[4] Beilvert A, Cormode DP, Chaubet F, et al. Tyrosine polyethylene glycol (PEG)-micelle magnetic resonance contrast agent for the detection of lipid rich areas in atherosclerotic plaque. Magn Reson Med 2009;62:1195–201.
[5] Kabalka G, Buonocore E, Hubner K, et al. Gadolinium-labeled liposomes: targeted MR contrast agents for the liver and spleen. Radiology 1987;163:255–8.
[6] McAteer MA, Sibson NR, von Zur Muhlen C, et al. In vivo magnetic resonance imaging of acute brain inflammation using microparticles of iron oxide. Nat Med 2007;13:1253–8.
[7] Tang TY, Muller KH, Graves MJ, et al. Iron oxide particles for atheroma imaging. Arterioscler Thromb Vasc Biol 2009;29:1001–8.
[8] Agrawal A, Huang S, Wei Haw Lin A, et al. Quantitative evaluation of optical coherence tomography signal enhancement with gold nanoshells. J Biomed Opt 2006;11:041121.
[9] Zagaynova EV, Shirmanova MV, Kirillin MY, et al. Contrasting properties of gold nanoparticles for optical coherence tomography: phantom, in vivo studies and Monte Carlo simulation. Phys Med Biol 2008;53:4995–5009.
[10] Kirillin M, Shirmanova M, Sirotkina M, et al. Contrasting properties of gold nanoshells and titanium dioxide nanoparticles for optical coherence tomography imaging of skin: Monte Carlo simulations and in vivo study. J Biomed Opt 2009;14:021017.
[11] Lee TM, Oldenburg AL, Sitafalwalla S, et al. Engineered microsphere contrast agents for optical coherence tomography. Opt Lett 2003;28:1546–8.
[12] Ramos CL, Huo Y, Jung U, et al. Direct demonstration of P-selectin- and VCAM-1-dependent mononuclear cell rolling in early atherosclerotic lesions of apolipoprotein E-deficient mice. Circ Res 1999;84:1237–44.
[13] Kunkel EJ, Jung U, Bullard DC, et al. Absence of trauma-induced leukocyte rolling in mice deficient in both P-selectin and intercellular adhesion molecule 1. J Exp Med 1996;183:57–65.
[14] Choudhury RP, Fisher EA. Molecular imaging in atherosclerosis, thrombosis, and vascular inflammation. Arterioscler Thromb Vasc Biol 2009;29:983–91.
[15] Wijesurendra RS, Jefferson A, Choudhury RP. Target: ligand interactions of the vascular endothelium, implications for molecular imaging in inflammation. Integr Biol (Camb) 2010;2:467–82.
[16] McAteer MA, Schneider JE, Ali ZA, et al. Magnetic resonance imaging of endothelial adhesion molecules in mouse atherosclerosis using dual-targeted microparticles of iron oxide. Arterioscler Thromb Vasc Biol 2008;28:77–83.
[17] Pfaffl MW. A new mathematical model for relative quantification in real-time RT-PCR. Nucleic Acids Res 2001;29, e45.
[18] Jebelovszki E, Kiraly C, Erdei N, et al. High-fat diet-induced obesity leads to increased NO sensitivity of rat coronary arterioles: role of soluble guanylate cyclase activation. Am J Physiol 2008;294:H2558–64.
[19] Koller A, Bagi Z. Nitric oxide and H_2O_2 contribute to reactive dilation of isolated coronary arterioles. Am J Physiol 2004;287:H2461–7.
[20] Bagi Z, Koller A, Kaley G. Superoxide–NO interaction decreases flow- and agonist-induced dilations of coronary arterioles in type 2 diabetes mellitus. Am J Physiol 2003;285:H1404–10.
[21] Skala MC, Crow MJ, Wax A, Izatt JA. Photothermal optical coherence tomography of epidermal growth factor receptor in live cells using immunotargeted gold nanospheres. Nano Lett 2008;8:3461–7.
[22] Farkas S, Hornung M, Sattler C, et al. Blocking MAdCAM-1 in vivo reduces leukocyte extravasation and reverses chronic inflammation in experimental colitis. Int J Colorectal Dis 2006;21:71–8.
[23] Bhatia SK, King MR, Hammer DA. The state diagram for cell adhesion mediated by two receptors. Biophys J 2003;84:2671–90.
[24] Eniola AO, Willcox PJ, Hammer DA. Interplay between rolling and firm adhesion elucidated with a cell-free system engineered with two distinct receptor–ligand pairs. Biophys J 2003;85:2720–31.
[25] Shimizu Y, Newman W, Gopal TV, et al. Four molecular pathways of T cell adhesion to endothelial cells: roles of LFA-1, VCAM-1, and ELAM-1 and changes in pathway hierarchy under different activation conditions. J Cell Biol 1991;113:1203–12.
[26] Marin V, Montero-Julian FA, Gres S, et al. The IL-6-soluble IL-6R alpha autocrine loop of endothelial activation as an intermediate between acute and chronic inflammation: an experimental model involving thrombin. J Immunol 2001;167:3435–42.
[27] Otto M, Bittinger F, Kriegsmann J, Kirkpatrick CJ. Differential adhesion of polymorphous neutrophilic granulocytes to macro- and microvascular endothelial cells under flow conditions. Pathobiology 2001;69:159–71.

[28] Richter U, Schroder C, Wicklein D, et al. Adhesion of small cell lung cancer cells to E- and P-selectin under physiological flow conditions: implications for metastasis formation. Histochem Cell Biol 2011;135:499–512.
[29] Kelly KA, Allport JR, Tsourkas A, et al. Detection of vascular adhesion molecule-1 expression using a novel multimodal nanoparticle. Circ Res 2005;96: 327–36.
[30] Nahrendorf M, Jaffer FA, Kelly KA, et al. Noninvasive vascular cell adhesion molecule-1 imaging identifies inflammatory activation of cells in atherosclerosis. Circulation 2006;114:1504–11.
[31] Oh J, Feldman MD, Kim J, et al. Detection of macrophages in atherosclerotic tissue using magnetic nanoparticles and differential phase optical coherence tomography. J Biomed Opt 2008;13:054006.